

# Journal of Materials Chemistry A

Accepted Manuscript



This is an *Accepted Manuscript*, which has been through the Royal Society of Chemistry peer review process and has been accepted for publication.

*Accepted Manuscripts* are published online shortly after acceptance, before technical editing, formatting and proof reading. Using this free service, authors can make their results available to the community, in citable form, before we publish the edited article. We will replace this *Accepted Manuscript* with the edited and formatted *Advance Article* as soon as it is available.

You can find more information about *Accepted Manuscripts* in the [Information for Authors](#).

Please note that technical editing may introduce minor changes to the text and/or graphics, which may alter content. The journal's standard [Terms & Conditions](#) and the [Ethical guidelines](#) still apply. In no event shall the Royal Society of Chemistry be held responsible for any errors or omissions in this *Accepted Manuscript* or any consequences arising from the use of any information it contains.

Cite this: DOI: 10.1039/c0xx00000x

www.rsc.org/xxxxxx

ARTICLE TYPE

## Work-function tunable Polyelectrolyte Complex (PEI:PSS) as Cathode Interfacial Layer for Inverted Organic Solar Cells

Zhenhua Lin,<sup>a,c</sup> Jingjing Chang,<sup>b,c</sup> Jie Zhang,<sup>c</sup> Changyun Jiang,<sup>c\*</sup> Jishan Wu,<sup>b,c\*</sup> and Chunxiang Zhu<sup>a\*</sup>

Received (in XXX, XXX) Xth XXXXXXXXX 20XX, Accepted Xth XXXXXXXXX 20XX

DOI: 10.1039/b000000x

High-efficiency inverted polymer solar cells (PSCs) with polyelectrolyte complex, polyethylenimine:poly(styrenesulfonate) (PEI:PSS), as the cathode interfacial layer for efficient electron extractions is demonstrated. By introducing the negatively charged PSS<sup>-</sup> as the counter ions into PEI, the imine protonation could be tuned, leading to tunable work-function of the PEI:PSS coated ITO. The incorporation of PSS in PEI enhances the photocurrent and power conversion efficiency (PCE) of the devices, due to an improved electron extraction at the PEI:PSS/active-layer interfaces. Furthermore, a TiO<sub>x</sub>/PEI:PSS combined interfacial layer further enhances the cell performance and eliminates the need for light-soaking treatment for TiO<sub>x</sub>, owing to the improved hole-blocking and surface-states passivation in the interfacial layer. The achieved high cell performance, better stability, low-cost materials, and low-temperature solution processes of the TiO<sub>x</sub>/PEI:PSS interfacial layers demonstrate a promising cathode configuration for realizing efficient and long lifetime PSCs.

### Introduction

Inverted structural polymer solar cells (PSCs),<sup>[1-3]</sup> which use indium-tin-oxide (ITO) substrate as the cathode and a high-work-function metal such as silver or gold as the top anode, have been considered as an advantageous approach for improving the device air stability. Usually, an additional interfacial layer between the ITO cathode and organic active layer is introduced in an inverted PSC.<sup>[4-7]</sup> This is because the high work function of the bottom ITO cathode usually hampers the formation of ohmic contact for electron transport from the active layer to the ITO cathode. Thus, an interfacial layer is added in between the ITO and active layer to reduce or eliminate the electron-extraction barrier.<sup>[8-10]</sup>

Several metal oxides have been investigated and applied for the cathode interfacial layer in inverted PSCs, such as zinc oxide (ZnO),<sup>[4-5]</sup> titanium oxide (TiO<sub>x</sub>),<sup>[6-7]</sup> owing to their high transparency, efficient electron extraction and hole blocking capability. However, there are intrinsic limitations in these devices with metal oxides as the interfacial layer, such as the high rate of trap-assisted recombination on the interfacial layer,<sup>[11-12]</sup> and inherent incompatibility between the inorganic metal oxides and organic active layer.<sup>[13-15]</sup> Meanwhile, devices with ZnO for the interfacial layer usually suffer from a significant photo-induced degradation during the exposure of light,<sup>[16]</sup> and the devices with TiO<sub>x</sub> film as the interfacial layer usually need post-light soaking (or UV treatment) to improve the performance.<sup>[6]</sup>

Organic thin films based on alcohol or water soluble polyelectrolyte materials, such as poly[(9,9-bis(3'-(N,N-dimethylamino)propyl)-2,7-fluorene)-alt-2,7-(9,9-dioctylfluorene)] (PFN),<sup>[8]</sup> poly(ethylene oxide) (PEO),<sup>[9]</sup> polyallylamine (PAA)<sup>[10]</sup> and polyethylenimine (PEI),<sup>[10]</sup> have been successfully employed for forming the interfacial layer on

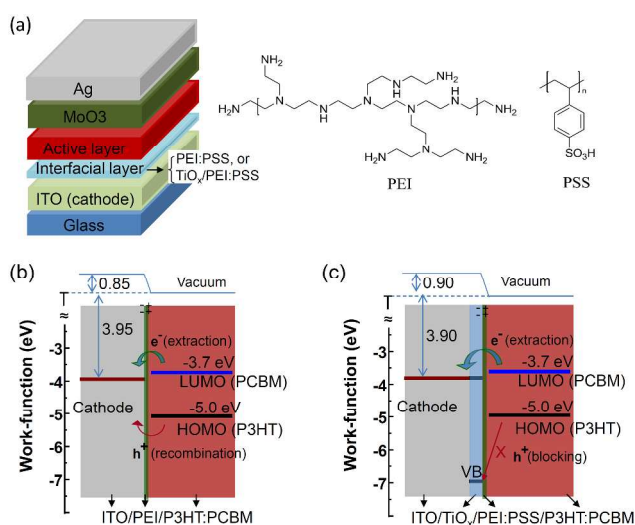
ITO for inverted PSCs. These polymer layers can lower the work function of ITO cathode and facilitate the collections of photogenerated charge-carriers by forming interfacial dipoles.<sup>[17-18]</sup> Among these, conjugated polyelectrolytes (CPEs) as candidates for the interfacial layer are becoming the focus of research interest because they possess also organic semiconducting properties and good solution processability.<sup>[19]</sup> Recently, the zwitterionic conjugated polyelectrolytes (ZCPEs) as interfacial layers showed superior performance than their corresponding cationic CPEs because the unwanted space charges of the mobile counterions in the latter are prevented in the former by using zwitterions with no mobile ions.<sup>[20-22]</sup> However, most of the CPEs are complicated to synthesize, while developing suitable and high performance ZCPEs are still on the way.

Non-conjugated polyelectrolyte like PEI has been used for the cathode interfacial layer for PSCs and realized good cell performance.<sup>[23]</sup> PEI is a cationic polymer which is commercially available. It is cost-effective, stable in aqueous solutions, and also suitable for solution process at low temperature, which is desirable for large-area printing solar cells. Meantime, it can use water as the solvent which is environment friendly. However, the bare PEI polymer is insulting with very low conductivity, and a PEI interfacial layer produces either a high series resistance in a thicker film (e.g. ~10 nm) or inefficient coverage/adsorption on the ITO surface in an ultra thin film (e.g. < 2 nm), which usually limits the photocurrent of the inverted PSCs.

In this work, we introduce immobile negatively charged poly(styrenesulfonate) (PSS) into PEI to form a high performance cathode interfacial layer for realizing PSC with high efficiency and better stability. Negatively charged PSS<sup>-</sup> is good candidate as the counter ions to PEI due to its good solubility in water, weak acidic nature to enhance the protonation, and good

film-forming properties. Compared to PEI-only as the interfacial layer, the PEI:PSS interlayer resulted in significantly increased photocurrent and improved power conversion efficiency (PCE) from the cells with either poly(3-hexylthiophene):[6,6]-phenyl-5 C61-butyric acid methyl ester (P3HT:PC61BM) or poly[[9-(1-octylonyl)-9H-carbazole-2,7-diyl]-2,5-thiophenediyl-2,1,3-benzothiadiazole-4,7-diyl-2,5-thiophenediyl]: phenyl-C71-butyric acid methylester (PCDTBT: PC71BM) as the active layer. Furthermore, when a  $\text{TiO}_x$ /PEI:PSS bi-layer configuration was  
10 used as the interfacial layer, the device performance was further enhanced with improved device stability, and more importantly, it eliminated the need for post-UV treatment which is commonly used for low-temperature processed  $\text{TiO}_x$  interfacial layer, demonstrating a promising cathode configuration for PSCs.

## 15 Results and Discussion



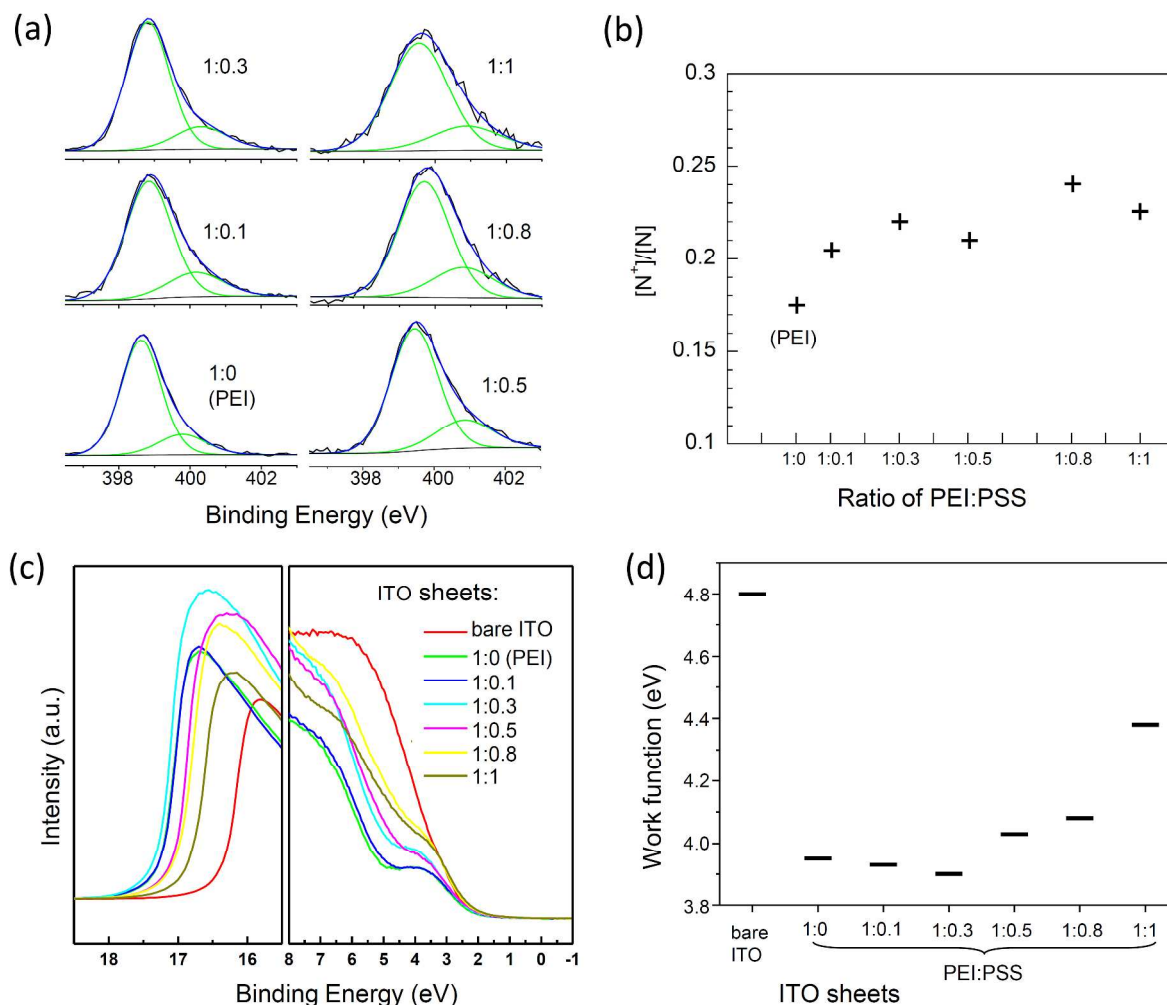
**Fig.1** Device structure of the inverted PSCs, and chemical structures of PEI and PSS (a), and proposed schemes for band alignment and charge transport processes (towards cathode) in the ITO/PEI:PSS/P3HT:PCBM junctions (b) and ITO/ $\text{TiO}_x$ /PEI:PSS/P3HT:PCBM junctions (c).

Fig. 1a illustrates device structure of the inverted PSCs and the chemical structures of PEI and PSS. When PEI or PEI:PSS aqueous solutions are deposited on ITO films, the positively charged amines (protonated amines) of PEI:PSS interact strongly with the negatively charged terminal oxygen ions on the ITO surface to form an ultrathin surface layer on ITO. Thus the existence of protonated amines may be a key factor affecting the forming and uniformity of the interfacial layer, cathode work-function and hence the device performance.<sup>[10, 24-25]</sup> Since the imine protonation could make the PEI solution more basic, studies on the pH values and the electrical conductivity of the PEI:PSS solutions can help us understanding the imine protonation situations in the solution. The relationships of the measured pH value and conductivity of the solutions to the PEI:PSS ratio are presented in Fig. S1 (see SI). It shows that the pH value increases first with increasing PSS content, from 10.26 at PEI-only to 11.10 at PEI:PSS = 1:0.8. This indicates increased imine protonation in the solution with increasing PSS content.

However, much higher PSS content at PEI:PSS = 1:1 has a decreased pH value which is due to excess PSS (PH = 4.5). One more point need to be mentioned is that the basic nature of PEI:PSS could avoid the acidizing effect encountered in PEDOT:PSS/ITO system. The solution conductivity (as shown in Fig. S1) increased significantly with the increase of PSS content, from 13.3 mS/m (PEI-only) to 224.5 mS/m (PEI:PSS =1:1) which is also much higher than that of the pure PSS solution (91.0 mS/m), demonstrating again the increased protonated ions in the solutions with higher PSS ratio.

XPS measurements were carried out to analyze the amines protonation situations in the surface layers on ITO. Fig. 2a shows the high-resolution XPS spectra of N 1s of the PEI:PSS films on ITO with different PEI:PSS ratios of 1:0 (PEI-only), 1:0.1, 1:0.3, 1:0.5, 1:0.8 and 1:1. It is clearly shown that the N 1s peaks exhibit at binding energy of 399.5 eV and 401 eV which are corresponding to the nitrogen atom in neutral amines (N) and protonated amines ( $\text{N}^+$ ), respectively.<sup>[26-28]</sup> The  $[\text{N}^+]/[\text{N}]$  ratio of each sample has been quantitatively analyzed as shown in Fig. 2b. It can be seen that all the ITO/PEI:PSS films have higher  $[\text{N}^+]/[\text{N}]$  ratios compared to that of ITO/PEI. The  $[\text{N}^+]/[\text{N}]$  increases first with the increase of PSS ratio from 0, 0.1 to 0.3, and then gradually saturate with further increase of the PSS content. High  $[\text{N}^+]/[\text{N}]$  ratio should facilitate the intimate interaction between the PEI:PSS layer and ITO to form more uniform interfacial layer. In the meantime, the acid group in PSS<sup>-</sup> interacts with the protonated amines forming a negatively charged surface thus may further influence the ITO work-function and the electric properties of the interfaces between the PEI:PSS layer and active layer. It is also seen that with increased  $[\text{N}^+]/[\text{N}]$  ratio, the binding energy of the N 1s peaks shifts to the higher value, indicating possible changes of the work-functions of the ITO films.

The work function changes of the ITO sheets modified with PEI:PSS were investigated by UPS. Fig.2c shows the second cutoff edges of the UPS spectra of a bare-ITO sheet and ITO/PEI:PSS sheets with different PEI:PSS ratios, and the work-functions of these ITO sheets were calculated and shown in Fig. 2d. It shows that the work-functions of all the ITO/PEI:PSS (including ITO/PEI) films decreased largely as compared to the bare ITO, which is mainly caused by forming the molecular and interfacial dipoles on the ITO surface.<sup>[10, 23]</sup> The work-function (3.95 eV) of ITO/PEI (PEI:PSS=1:0) shows a reduction of 0.85 eV as compared to that of the bare-ITO (4.80 eV). When small amount of PSS is added into PEI (e.g. PSS = 0.1 and 0.3), the work-function was slightly further reduced with that of 3.90 eV observed at PEI:PSS = 1:0.3. The further reduction in the work-function with small PSS contents is most possibly the result of the increased protonated amines ( $[\text{N}^+]$ ) (see fig. 2b). When the PSS ratio is increased to 0.5 and above, the work-function is gradually increased with the PSS content. This is because that the total amount of amines (of PEI) was largely decreased at high PSS ratio. This result indicates that the ITO/PEI:PSS work function can be tuned in between 3.90 eV to 4.40 eV by varying the PSS/PEI ratio from 1:0 to 1:1. Based on the above studies, the ITO/PEI:PSS (1:0.3) is showing as an optimum configuration for the cathode of inverted PSCs.



**Fig.2** (a) High-resolution XPS spectra of N 1s and (b)  $[N^+]/[N]$  ratios of the PEI:PSS films on ITO with different PEI:PSS ratios of 1:0 (PEI only), 1:0.1, 1:0.3, 1:0.5, 1:0.8, and 1:1; (c) UPS spectra and (d) Work Functions of the ITO and ITO/PEI:PSS sheets with different PEI:PSS ratios.

The optical and morphological properties of the ITO substrates coated with different cathode interfacial layers have also been investigated. The transmittances of the ITO/PEI:PSS films are almost identical to that of the bare ITO film (see Fig. S2 in SI). The surface roughness of the ITO/PEI:PSS films are also very close to that of the bare ITO, as characterized by AFM (see Fig. S3).

To explore the impacts of the PEI:PSS interfacial layers on the PSC device performance, inverted PSCs with ITO/PEI and ITO/PEI:PSS (1:0.3) as the cathodes were fabricated. For comparison, PSC devices using bare ITO, ITO/ZnO and ITO/TiO<sub>x</sub> as the cathodes were also fabricated. The cells performance of open circuit voltage ( $V_{oc}$ ), short circuit current ( $J_{sc}$ ), fill factor (FF) and PCE, and the cells' series ( $R_s$ ) and shunt resistance ( $R_{sh}$ ) are summarized in Table 1. It can be seen from Table 1 that the  $J_{sc}$  of the PEI-based cell is only 8.62 mA/cm<sup>2</sup>, while it is increased significantly to 10.30 mA/cm<sup>2</sup> with the incorporation of PSS into PEI in the cell based on PEI:PSS (1:0.3). The  $V_{oc}$  and FF of the PEI:PSS based cell (0.60V, 60%)

are also slightly higher than that of the PEI based cell ( $V_{oc}$ =0.59V, FF=59%). As a consequence, the PEI:PSS-based cell showed significantly increased PCE (3.68%) as compared to the PEI-based cell (3.01%). It can also be observed that the PEI:PSS-based cell has considerably decreased  $R_s$  (8.6  $\Omega$ /cm<sup>2</sup>) and increased  $R_{sh}$  (720  $\Omega$ /cm<sup>2</sup>) as compared to the PEI-based cell ( $R_s$  =10.6  $\Omega$ /cm<sup>2</sup>,  $R_{sh}$  = 546  $\Omega$ /cm<sup>2</sup>). It has to be point out that the concentration of the polyelectrolyte solution was optimized, and it was found that slightly lower concentration can give higher performance, but with poor reproducibility due to high chance of electrical short. Incident photon-to-current conversion efficiency (IPCE) spectra of the devices with the ZnO, PEI and PEI:PSS interfacial layers are shown in Fig. 3. The IPCE at the wavelength of 550 nm is about 73 % for the PEI:PSS based device, which is much higher than that of the PEI-based device (65% at 550 nm). The higher  $J_{sc}$  and lower  $R_s$  of the PEI:PSS based cell indicates a lower resistance and higher efficiency for electron extractions from the active layer to cathode. Since both PEI and PSS are non-conjugated polymers, and the work-functions of ITO/PEI and

ITO/PEI:PSS (1:0.3) electrodes have not showed a significant difference, thus it is reasonable to ascribe the improvement of electron extractions to an improved P3HT:PCBM/PEI:PSS interfaces by incorporation of the PSS, despite the mechanism for electron transport/injection through such interfacial layer is still unclear,

The PEI:PSS-based cell also showed higher  $J_{sc}$  (10.30

$\text{mA}/\text{cm}^2$ ) and  $V_{oc}$  (0.60 V) than that of the ZnO-based cell (9.46  $\text{mA}/\text{cm}^2$ , 0.56V) and  $\text{TiO}_x$ -based cell (9.97  $\text{mA}/\text{cm}^2$ , 0.55V). The considerable increase of the  $V_{oc}$  suggests a reduced cathode work-function and recombination rate in the PEI:PSS-based device as compared to the metal-oxide-based devices. This is mainly because of a higher rate of trap-assisted recombination on the metal-oxide surfaces.<sup>[11-12]</sup>

15

**Table 1.** Device performance data of the inverted P3HT:PC<sub>61</sub>BM solar cells incorporating different interfacial layers on ITO cathodes.

Interfacial layer	$J_{sc}$ ( $\text{mA}/\text{cm}^2$ )	$V_{oc}$ (V)	FF (%)	$\eta^*$ (%)	$R_s$ ( $\Omega/\text{cm}^2$ )	$R_{sh}$ ( $\Omega/\text{cm}^2$ )
No	8.29	0.30	37	0.92	25.0	73
PEI	8.62	0.59	59	3.01	10.6	546
PEI:PSS (1:0.3)	10.30	0.60	60	3.68	8.6	720
ZnO	9.46	0.56	59	3.12	9.7	900
$\text{TiO}_x$	9.97	0.55	53	2.90	13.1	1059
$\text{TiO}_x/\text{PEI:PSS}(1:0.3)$	9.89	0.60	66	3.91	7.8	2223

\* Device performances are reproducible with reasonable variations ( $\leq 5\%$ ) (See Fig. S6).

**Table 2.** Device performance data of inverted PCDTBT:PC<sub>71</sub>BM solar cells incorporating  $\text{TiO}_x$ , PEI, PEI:PSS(1:0.3) and  $\text{TiO}_x/\text{PEI:PSS}(1:0.3)$  films as the cathode interfacial layer.

Interfacial layer	$J_{sc}$ ( $\text{mA}/\text{cm}^2$ )	$V_{oc}$ (V)	FF (%)	$\eta^*$ (%)	$R_s$ ( $\Omega/\text{cm}^2$ )	$R_{sh}$ ( $\Omega/\text{cm}^2$ )
$\text{TiO}_x$	9.62	0.87	58	4.85	19.1	900
PEI	8.83	0.83	53	3.88	13.1	562
PEI:PSS (1:0.3)	10.19	0.88	56	5.02	9.3	640
$\text{TiO}_x/\text{PEI:PSS}(1:0.3)$	9.73	0.90	61	5.34	8.1	973

\* Device performances are reproducible with reasonable variations ( $\leq 5\%$ ) (See Fig. S6).

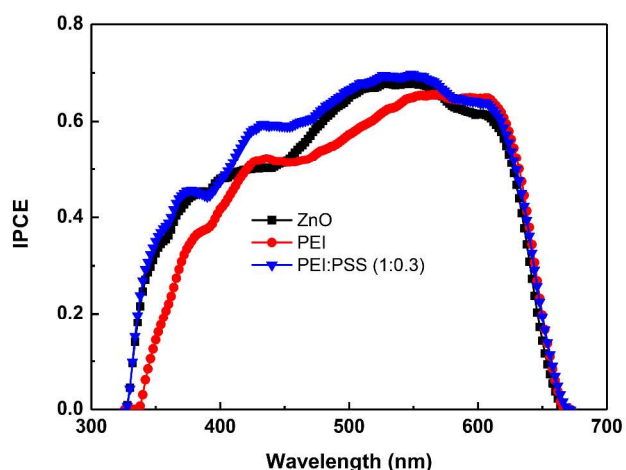


Fig. 3 IPCE spectra of the inverted P3HT:PC<sub>61</sub>BM solar cells with ZnO, PEI and PEI:PSS (1:0.3) cathode interfacial layers.

Using metal-oxide/CPE bilayer structure as the cathode interlayer has recently been demonstrated to be an efficient way to enhance the performance of optoelectronic devices.<sup>[15]</sup> Since the PEI:PSS layer is very thin, it might be not efficient to block hole collection to the cathode as schematically shown in Fig.1b of the holes ( $h^+$ ) transporting from the highest occupied molecular orbit (HOMO) of P3HT to the ITO cathode, leading to recombination (loss) of charges at the cathode/active-layer

interface. Thus, we further incorporated a combination of  $\text{TiO}_x$  (15nm) and PEI:PSS (1:0.3) as the interfacial layer for inverted cells, in expectation to further improve the hole blocking in the interlayer. As shown in Fig. 1c, a  $\text{TiO}_x$  layer (15 nm) with much lower valence band ( $VB \approx -7.6$  eV) will efficiently block the holes ( $h^+$ ) transporting from the P3HT-HOMO to ITO cathode. Here, low temperature solution processed  $\text{TiO}_x$  thin film was used for the interfacial layer because it has been proved to be a dense and stable electron transport layer with efficient hole blocking capability,<sup>[6,15,29]</sup> and very importantly, the fabrication process is compatible with plastic substrates and roll-to-roll methods. Fig. 4 compares the  $J - V$  characteristics of a  $\text{TiO}_x$  based device and a  $\text{TiO}_x/\text{PEI:PSS}(1:0.3)$  based device (the performance data are also presented in table 1). A light soaking is usually needed for devices with  $\text{TiO}_x$  cathode interfacial layer, to improve the electric properties of the interfacial layer.<sup>[6, 30]</sup> It can be seen from Fig. 4 and table 1 that the  $J - V$  curve of the  $\text{TiO}_x$ -based cell before light soaking has a kink (S shape), and the kink is removed after light soaking for 10 min, with PCE of 2.90% obtained. However, the  $\text{TiO}_x/\text{PEI:PSS}$ -based cell, with the combination of  $\text{TiO}_x$  and PEI:PSS (1:0.3) interlayer, eliminated the S shape in the  $J - V$  curve (no light soaking needed) and also enhanced the PCE to 3.91% which is higher than that of both the  $\text{TiO}_x$ -based cell (2.90%) and PEI:PSS (1:0.3) based cell (3.68%). The PCE increase is resulted from the increases in  $V_{oc}$  and FF. The elimination of S shape in the  $J - V$  curve of the  $\text{TiO}_x/\text{PEI:PSS}$ -based device indicates that the combination of PEI:PSS with the

TiO<sub>x</sub> layer, similar to undergoing light soaking, led to increased conductivity and lower work-function (higher Fermi level) of the TiO<sub>x</sub> layer,<sup>[6,30]</sup> which eliminating the energy barriers at the TiO<sub>x</sub>/active-layer interfaces for electron injection and transport. This can also be evidenced from the much lower R<sub>s</sub> of the TiO<sub>x</sub>/PEI:PSS-based cell (7.8 Ω/cm<sup>2</sup>) as compared to the TiO<sub>x</sub>-based cell (13.1 Ω/cm<sup>2</sup>).

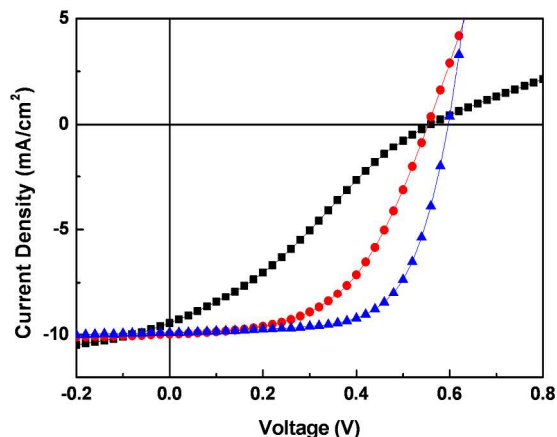


Fig. 4 *J* - *V* characteristics of inverted P3HT:PC<sub>61</sub>BM solar cells with TiO<sub>x</sub> interface layer before (square) and after (circle) light soaking, and with TiO<sub>x</sub>/PEI:PSS interface layer (without light soaking) (triangle).

As seen from table 1, the *V*<sub>oc</sub> of TiO<sub>x</sub>/PEI:PSS-based cell (0.60V) is higher than that of the TiO<sub>x</sub>-based cell (0.55V) but similar to that of the PEI:PSS-based cell (0.60V), indicating that the TiO<sub>x</sub> surface was passivated with PEI:PSS thus avoiding trap-assisted recombination at the TiO<sub>x</sub>/active-layer interfaces. Significantly increased FF (66%) and *R*<sub>sh</sub> (2223 Ω/cm<sup>2</sup>) were obtained from the TiO<sub>x</sub>/PEI:PSS-based cell, which are higher than that of both the TiO<sub>x</sub>-based cell (FF=53%, *R*<sub>sh</sub>=1059 Ω/cm<sup>2</sup>) and PEI:PSS-based cell (FF=60%, *R*<sub>sh</sub>=720 Ω/cm<sup>2</sup>). This indicates that the carriers recombination through the TiO<sub>x</sub>/PEI:PSS interlayer was reduced as compared to that through the PEI:PSS(1:0.3) interlayer, which should be resulted from the improved hole blocking by the TiO<sub>x</sub>/PEI:PSS combination, as expected, to prevent the collection of holes to the cathode (see the scheme in Fig. 1c).

The stability of P3HT:PC<sub>61</sub>BM solar cells using PEI:PSS interfacial layers has also been investigated. The stability of the inverted solar cells were checked by following the procedure of ISOS-D-1 Shelf.<sup>[31]</sup> The normalized PCEs as a function of storage time of the cells (unencapsulated) in nitrogen filled glove box are shown in Fig. 5. The PCE of ZnO-based cell has the faster degradation, with only 62% remaining after 180 days. The PCEs of PEI-, and PEI:PSS-based cells have similarly the slowest degrading trend indicating much improved stability. The PCEs remained at approximately 94% of the origin values after 180 days for the PEI:PSS (1:0.3)-based cell. For the cells based on TiO<sub>x</sub> and TiO<sub>x</sub>/PEI:PSS (1:0.3), the PCEs remained at approximately 93% and 90%, respectively, both exhibit better stability than ZnO-based cell. Since the TiO<sub>x</sub> film is air stable and robust, the TiO<sub>x</sub>/PEI:PSS configuration is showing a good candidate for the interfacial layer with both high performance and good air stability.

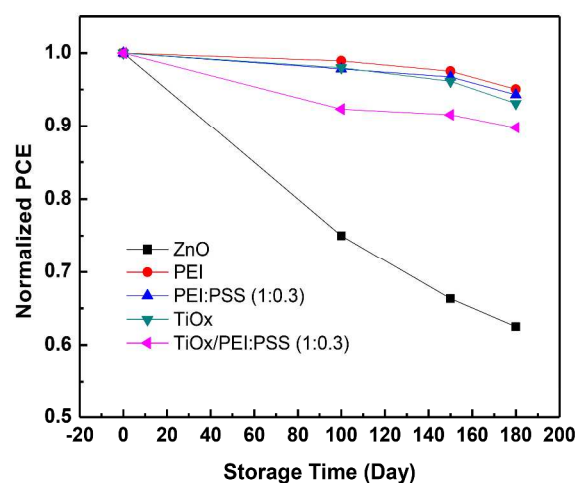


Fig. 5 Stability of inverted P3HT:PC<sub>61</sub>BM solar cells with ZnO, PEI, PEI:PSS, TiO<sub>x</sub> and TiO<sub>x</sub>/PEI:PSS interfacial layers. For the TiO<sub>x</sub>-based cell, light soaking had been done before each measurement.

The PEI:PSS system was also applied to PCDTBT/PC<sub>71</sub>BM-based inverted PSCs to test its feasibility in more general material systems. Table 2 is the summary of the cell performances of inverted solar cells based on PCDTBT/PC<sub>71</sub>BM incorporating with TiO<sub>x</sub>, PEI, PEI:PSS(1:0.3), and TiO<sub>x</sub>/PEI:PSS(1:0.3), respectively, as the cathode interfacial layers (the J-V characteristics are shown in fig. S5). PCE of 5.02 % for PEI:PSS (1:0.3) based cell was obtained which is higher than that of the cells based on TiO<sub>x</sub> (4.85%) and PEI (3.88%). The PCE enhancement is mainly due to the increase in *J*<sub>sc</sub>. By using TiO<sub>x</sub>/PEI:PSS (1:0.3) combined interlayer, the PCE is further increased to 5.34% due to the further enhancement of *V*<sub>oc</sub> and FF, and again, light-soaking was avoided.

## Experimental details

ITO-coated glass substrates were cleaned by a routine solvent ultrasonic cleaning, sequentially with detergent, water, acetone, and iso-propanol (IPA) in an ultrasonic bath for 15 minutes each. For the PEI:PSS layer preparation, first, PEI (Mw ~25,000, from Sigma-Aldrich) and PSS (Mw ~70,000, from Sigma-Aldrich) with different ratios (1:0.1, 1:0.3, 1:0.5, 1:0.8 and 1:1) were directly dissolved in de-ionized water, and with a controlled concentration (2 mg/mL). PEI only solution (2 mg/mL) was also prepared as the reference. The solution was stirred overnight to yield a homogenous, clear, and transparent solution. After the solutions were prepared, PEI and PEI:PSS layers were formed by spin-coating the solutions on the top of ITO or TiO<sub>x</sub>-coated ITO substrates at 4000 rpm for 1 min and immediately annealed at 110 °C for 10 min. To fabricate the metal-oxide interfacial layers, ZnO thin films were fabricated on ITO by spin coating a solution with 0.1 M ZnO powders (Sigma Aldrich) dissolved in ammonia solution. The ZnO films were spin coated at 3000 rpm for 30s, then annealing at 120 °C for 10 min in air. The TiO<sub>x</sub> thin films were fabricated by dissolving titanium isopropoxide (Sigma Aldrich) in IPA with 1:200 volume ratio, and then the thin films were spin coated at 3000 rpm for 60 s followed by annealing at 120 °C for 10 min in air. The thickness of the resulted TiO<sub>x</sub> film

is 15-20nm. Following that, an active layer was deposited on top of the surface modified ITO substrates (including bare-ITO, ITO/PEI, ITO/PEI:PSS, ITO/ZnO, ITO/TiO<sub>x</sub> and ITO/TiO<sub>x</sub>/PEI:PSS) by spin-coating a solution of the P3HT (Rieke Metals) and PC<sub>61</sub>BM (Nano-C) blend with a weight ratio of 1:1 in 1, 2-dichlorobenzene (20 mg/ml) at 500 rpm for 130 s in N<sub>2</sub> environment. The active layers were dried for 2 hours and then annealed at 140 °C for 10 minutes. Another type of active layer was deposited by spin-coating a solution of the PCDTBT (1-Materials) and PC<sub>71</sub>BM (Nano-C) blend with a weight ratio of 1:1 in 1, 2-dichlorobenzene: chlorobenzene (3:1) (7 mg/ml) at 1000 rpm for 100 s in N<sub>2</sub> environment. The active layers were dried at room temperature for 1 hour and then at 70 °C for 10 minutes. Finally, a MoO<sub>3</sub> layer (6 nm) and an Ag layer (100 nm) were deposited on the active layer by using vacuum thermal evaporation. A metal shadow mask was used for the Ag deposition to define the device area of 9 mm<sup>2</sup>.

The current density – voltage ( $J - V$ ) characteristics of the devices were measured using a Keithley 2400 parameter analyzer in the dark and under a simulated light (AM 1.5G) with intensity of 100 mW/cm<sup>2</sup> calibrated by silicon reference cell. IPCE measurements were performed under short-circuit conditions with a lock-in amplifier (SR510, Stanford Research System) at a chopping frequency of 280 Hz during illumination with a monochromatic light from an arc lamp. The pH values of the PEI:PSS solutions were tested by the AB15 pH meter (Accumet Basic) at room temperature (25 °C). The conductivity of the PEI:PSS solutions were measured by pH/ION/COND meter (F-74BW LAQUA) at room temperature (25 °C). Physical properties of the PEI:PSS film were characterized by X-ray photoelectron spectroscopy (XPS) (VG ESCALAB-220i XL) and ultraviolet photoelectron spectroscopy (UPS) (VG ESCALAB-220i XL). The transmittance spectra of the PEI:PSS films deposited onto ITO/glass were characterized using an UV-3600 Shimadzu UV-VIS-NIR Spectrophotometer. The surface morphology and the roughness of the PEI:PSS film deposited on ITO/glass substrate were observed by tapping-mode Atomic Force Microscopy (TM-AFM) which was performed on a Bruker ICON-PKG atomic force microscopy (AFM).

## Conclusions

In conclusion, high-efficiency inverted organic solar cells incorporating non-conjugated polyelectrolyte complex PEI:PSS as the cathode interfacial layer have been successfully demonstrated. It was found that the incorporation of PSS in PEI can further tune the ITO work-function by changing the amount of protonated amines in the interfacial layers. The incorporation of PSS in PEI enhanced the cell  $J_{sc}$ , owing to an improved electron extraction at the PEI:PSS/active-layer interfaces, and resulted in increased PCE (e.g. 3.68%) compared to that using PEI-only as interlayer (e.g. 3.01%). Moreover, the combined TiO<sub>x</sub>/PEI:PSS (1:0.3) interfacial layer further enhanced the FF due to better holes blocking and suppressed interface recombination, thus resulting in significantly increased PCE (3.91%) of the P3HT-PCBM devices, with no need for light soaking. Similarly, the PCE of the PCDTBT-PC<sub>71</sub>BM based cells was increased from 3.88% (with PEI) to 5.02% (with PEI:PSS) and 5.34% (with TiO<sub>x</sub>/PEI:PSS). The achieved high cell

performance, better stability, low-cost materials, and low-temperature solution process of the TiO<sub>x</sub>/PEI:PSS interfacial layer demonstrated a promising cathode configuration for realizing high efficiency and long lifetime PSCs.

## Acknowledgements

This work was financially supported by MOE Tier 2 grant (MOE2011-T2-2-130), and IMRE Core Funding (IMRE/13-1C0208, IMRE/13-1C0205).

[†] These authors contributed equally to this work.

## Notes and references

<sup>a</sup>Department of Electrical and Computer Engineering, National University of Singapore, 10 Kent Ridge Crescent, Singapore 119260,

Singapore, Email: [elezhucx@nus.edu.sg](mailto:elezhucx@nus.edu.sg)

<sup>b</sup>Department of Chemistry, National University of Singapore, 3 Science Drive 3, Singapore 117543, Singapore, Email: [chmwuj@nus.edu.sg](mailto:chmwuj@nus.edu.sg)

<sup>c</sup>Institute of Materials Research and Engineering, A\*STAR (Agency for Science, Technology and Research), 3 Research Link, Singapore 117602,

Singapore, Email: [jiangc@imre.a-star.edu.sg](mailto:jiangc@imre.a-star.edu.sg)

† Electronic Supplementary Information (ESI) available: PH value and conductivity of the PEI:PSS solutions, optical and morphological properties of the PEI:PSS interfacial layers on ITO substrates. See DOI: 10.1039/b000000x/

- S. K. Hau, H.-L. Yip, N. S. Baek, J. Zou, K. O'Malley and A. K.-Y. Jen, *Appl. Phys. Lett.*, 2008, **92**, 253301.
- L. M. Chen, Z. Hong, G. Li and Y. Yang, *Adv. Mater.* 2009, **21**, 1434.
- Z. Xu, L. M. Chen, G.W. Yang, C.H. Huang, J. Hou, Y. Wu, G. Li, C. S. Hsu and Y. Yang, *Adv. Funct. Mater.*, 2009, **19**, 1227.
- Z. Liang, Q. Zhang, O. Wiranwetchayan, J. Xi, Z. Yang, K. Park, C. Li and G. Cao, *Adv. Funct. Mater.*, 2012, **22**, 2194.
- Y. Sun, J. H. Seo, C. J. Takacs, J. Seifter and A. J. Heeger, *Adv. Mater.*, 2011, **23**, 1679.
- Z. Lin, C. Jiang, C. Zhu and J. Zhang, *ACS Appl. Mater. Interfaces*, 2013, **5**, 713.
- H. Sun, J. Weickert, H. C. Hesse and L. Schmidt-Mende, *Sol. Energy Mater. Sol. Cells*, 2011, **95**, 3450.
- Z. He, C. Zhong, S. Su, M. Xu, H. Wu and Y. Cao, *Nat. Photon.*, 2012, **6**, 591.
- F. L. Zhang, F. Sedar and O. Inganäs, *Adv. Mater.*, 2007, **19**, 1835.
- H. Kang, S. Hong, J. Lee and K. Lee, *Adv. Mater.*, 2012, **24**, 3005.
- J. Liu, S. Shao, B. Meng, G. Fang and Z. Xie, *Appl. Phys. Lett.*, 2012, **100**, 213906.
- A. Gadisa, Y. Liu, E. T. Samulski and R. Lopez, *Appl. Phys. Lett.*, 2012, **100**, 253903.
- Y.-M. Chang, W.-F. Sua and L. Wang, *Macromol. Rapid Commun.*, 2008, **29**, 1303.
- H. Choi, H. Cho, S. Song, H. Suh and S. Park, J. Y. Kim, *Phys. Chem. Chem. Phys.*, 2010, **12**, 15309.
- H. Choi, J. S. Park, E. Jeong, G.-H. Kim, B. R. Lee, S. O. Kim, M. H. Song, H. Y. Woo and J. Y. Kim, *Adv. Mater.*, 2011, **23**, 2759.
- A. Manor, E. A. Katz, T. Tromholt and F. C. Krebs, *Adv. Energy Mater.*, 2011, **1**, 836.
- C. He, C. Zhong, H. Wu, R. Yang, W. Yang, F. Huang, G. Bazan and Y. Cao, *J. Mater. Chem.*, 2010, **20**, 2617.
- J. H. Seo and T.-Q. Nguyen, *J. Am. Chem. Soc.*, 2008, **130**, 10042.
- A. Duarte, K. Y. Pu, B. Liu and G. C. Bazan, *Chem. Mater.*, 2011, **23**, 501.
- U. Scherf, *Angew. Chem. Int. Ed.*, 2011, **50**, 5016.
- A. Kumar, G. Pace, A. A. Bakulin, J. Fang, P. K. H. Ho, W. T. S. Huck, R. H. Friend and N. C. Greenham, *Energy Environ. Sci.*, 2013, **6**, 1589.
- D. A. Rider, B. J. Worfolk, K. D. Harris, A. Lalany, K. S. Shahbazi, M. D. Fleischauer, M. J. Brett and J. M. Buriak, *Adv. Funct. Mater.*, 2010, **20**, 2404.

- 23 Y. Zhou, C. F.-Hernandez, J. Shim, J. Meyer, A. J. Giordano, H. Li, P. Winget, T. Papadopoulos, H. Cheun, J. Kim, M. Fenoll, A. Dindar, W. Haske, E. Najafabadi, T. M. Khan, H. Sojoudi, S. Barlow, S. Graham, J.-L. Brédas, S. R. Marder, A. Kahn and B. Kippelen, *Science*, 2012, **336**, 327.
- 24 C. Peng, Y. Thio and R. Gerhardt, *J. Phys. Chem. C*, 2010, **114**, 9685.
- 25 A. K. Kyaw, D. H. Wang, V. Gupta, J. Zhang, S. Chand, G. C. Bazan and A. J. Heeger, *Adv. Mater.*, 2013, **25**, 2397.
- 26 R. Schlapak, D. Armitage, N. Saucedo-Zeni, G. Latini, H. J. Gruber, P. Mesquida, Y. Samotskaya, M. Hohage, F. Cacialli and S. Howorka, *Langmuir*, 2007, **23**, 8916.
- 27 Y. Chen, E. T. Kang, K. G. Neoh, S. L. Lim, Z. H. Ma and K. L. Tan, *Colloid Polym. Sci.*, 2001, **279**, 73.
- 28 E. Metwalli, D. Haines, O. Becker, S. Conzone and C. G. Pantano, *J. Colloid Interf. Sci.*, 2006, **298**, 825.
- 29 L. M. Chen, Z. Hong, G. Li and Y. Yang, *Adv. Mater.*, 2009, **21**, 1434.
- 30 J. Kim, G. Kim, Y. Choi, J. Lee, S. H. Park and K. Lee, *J. Appl. Phys.*, 2012, **111**, 114511.
- 31 M. O. Reese, S. A. Gevorgyan, M. Jørgensen, E. Bundgaard, S. R. Kurtz, D. S. Ginley, D. C. Olson, M. T. Lloyd, P. Morvillo, E. A. Katz, A. Elschner, O. Haillant, T. R. Currier, V. Shrotriya, M. Hermenau, M. Riede, K. R. Kirov, G. Trimmel, T. Rath, O. Inganäs, F. Zhang, M. Andersson, K. Tvingstedt, M. Lira-Cantu, D. Laird, C. McGuinness, S.(J.). Gowrisanker, M. Pannone, M. Xiao, J. Hauch, R. Steim, D. M. DeLongchamp, R. Rösch, H. Hoppe, N. Espinosa, A. Urbina, G. Yaman-Uzunoglu, J.-B. Bonekamp, A. J. J. M. van Breemen, C. Girotto, E. Voroshazi and F. C. Krebs, *Sol. Energy Mater. Sol. Cells*, 2011, **95**, 1253.